❒ 575

Analytical determination of load resistance value for MQ-series gas sensors: MQ-6 as case study

Ajiboye A. T., Opadiji J. F., Yusuf A. O., Popoola J. O.
Department of Computer Engineering, University of Ilorin, Ilorin, Nigeria

Article Info	ABSTRACT
	The MQ-series gas sensors are attractive candidates in the area of gas concentration sensing due to their high sensitivity and low cost. Even though the sensor circuit sensitivity and sensor power dissipation level both depend on load resistance, the process of the load resistance selection has not been well researched, hence the need for this study. The derivation of model equations for determining the sensor circuit sensitivity and sensor power dissipation is presented. The derived equations were used to investigate a typical scenario of MQ-6 gas sensor under the influence of liquified petroleum gas (LPG). The variation of sensitivity with load resistance and that of power dissipation with sensor resistance were parametrically investigated. The load resistance that yields maximum sensor circuit sensitivity with the maximum sensor power dissipation less than the set threshold is the candidate resistance for the sensor circuit. The 20 kΩ load resistance recommended for MQ-6 in the datasheet was authenticated in this study, yielding the maximum possible sensor circuit sensitivity and tolerable sensor power dissipation of 0.195 mV/ppm and 3.125×10^{-4} W, respectively. *This is an open access article under the <u>CC BY-SA</u> license.*

Corresponding Author:

Ajiboye A. T.
Department of Computer Engineering
University of Ilorin, Ilorin, Nigeria
Email: ajiboye.at@unilorin.edu.ng

1. INTRODUCTION

The MQ-series gas sensors are attractive candidates in the area of gas concentration sensing due to their high sensitivity and low cost. The metal oxide (MOXs) semiconductor gas Sensors, comprising MQ-series and others, have wide applications in gas concentration sensing and detection due to their high sensitivity and low cost [1, 2]. The MOX semiconductor gas sensor consists of a micro AL_2O_3 ceramic tube, a sensitive layer of tin dioxide (SnO_2), and Nickel-Chromium alloys which serve as a heater coil. This sensor has 6 pins, 4 out of which are for signal and electrodes, while the remaining 2 are for heating coils [3-5]. The tin dioxide (SnO_2) semiconductor is the sensor gas-sensitive portion [3, 4, 6, 7] which has low conductivity in clean air [8]. The principle of operation of these sensors is based on the variation of their resistance when they come in contact with the gas to be sensed [7, 9, 10]. The magnitude of the sensor output signal depends on the concentration and nature of the gas [6, 8, 11] and the type of metal oxide used for the sensor sensing surface [2, 12, 13]. The sensor is made up of two elements, namely the heating and sensing elements. These elements are normally powered independently either from the same or separate voltage source. The heater voltage will allow it to generate the required heat for maintaining the sensor in the active state while the sensor voltage will allow the sensor to convert the sensed gas concentration to an appropriate voltage level across the load resistor connected in series with the sensing element [5, 9, 12, 14]. Because of the characteristic of the

sensing element a simple electrical equivalent circuit can be used to convert the sensed gas concentration to a corresponding signal usually voltage across the load resistor [5, 8, 9, 11].

To calibrate MOX semiconductor gas sensors the following sensor parameters must be known: sensor activation voltage (V_{CC}), sensor electrical equivalent circuit output voltage (V_{RL}), the sensor resistance for referent gas concentration and environmental conditions (temperature and humidity) (R_O) [15], the sensor resistance (R_S) and load resistance (R_L) [3]. The value of R_O is not explicitly given in the sensor datasheet; therefore, it has to be determined experimentally [3]. In practice R_O must be determined for every sensor to be used because it is practically impossible to have similar gas sensors with the same value of R_O [16]. This is because it is also, practically impossible to secure the reproducibility and stability of this class of sensors as a result of the impossibility of keeping the consistency of the manufacturing environment, therefore, there is usually some variation in the sensor behaviour from one sensor to another and from one production batch to another [7, 10]. After the determination of R_O value, the sensor resistance at different gas concentrations value for various gases and different environmental conditions (temperature and relative humidity (RH)) can be determined [2]. It should be noted that the sensor circuit sensitivity and the sensor power dissipation are both functions of the load resistance.

Even though the sensor circuit sensitivity and sensor power dissipation level both depend on load resistance, the process of resistance selection has not fully investigated, and hence the need for this study. The air quality using MQ-2 gas sensor was monitored as reported in [17], using the 20 kΩ load resistance as given in the sensor datasheet. The air quality monitoring system developed by [3] consisted of three sensors which include an MQ-7 gas sensor. However, a default manufacturer circuit with a load resistance of 1 KΩ was employed in the study, which is outside the range of value (5-47 kΩ) recommended in the datasheet with no justification. MQ-2 gas sensor was used by [18] for air quality monitoring with a load resistance value of 5 KΩ which is subjected to variation depending on the gas concentration to give room for sensitivity adjustment [19]. Four MOX sensors, consisting of MQ-2, MQ-3, MQ-6, MQ-135, were used in [4] for the development of a real-time olfaction monitoring system with a 10 kΩ load resistance for each of the sensors without considering their characteristics. An air pollution monitoring system using a single MQ-2 gas sensor for sensing both CO and smoke was developed in [20], using a 20 kΩ load resistance recommended in the sensor datasheet. The clean air sensor resistance parameter for MQ-5 gas sensor was computed in [1], by placing the sensor in fresh air while measuring the sensor output voltage with the 20 kΩ load resistance. However, the selection of load resistance was not justified. MQ-2 and MQ-7 were used for sensing flammable gases and carbon monoxide respectively in a death-defying gas intelligent sensor system [5]. The load resistance used for both MQ-2 and MQ-7 sensors was 1 kΩ which is outside the range (5-47 kΩ) recommended in the sensor datasheet.

In different microcontroller-based LPG leakage concentration monitoring and control systems proposed by [21-28], the leakage gas concentration was sensed in these systems using MQ-4 [28], MQ-6 [22, 23, 26, 27], MQ-5 [24] and MQ-2 [21, 25] gas sensors. The selection of the load resistance in all these systems sensor circuits was not considered. It was pointed out in [12, 29] that the value of the load resistor should be selected in such a way as to optimize the alarm threshold value and keep the sensor power dissipation below the maximum allowable value. For some sensors, the manufacturer provides data on the value of load resistance to be used so that the resolution would be sufficient around the alarm point. It was pointed out in [21] that the load resistance should be wisely selected to improve sensor performance because a lower value will result in less sensitivity while a higher value will give less accuracy.

In most of the reviewed works, there is no concrete justification for the selection of the load resistance for the MQ-series gas sensor circuit aside from the claim that the selected value is as given in the sensor datasheet. Therefore, considering the dependence of the sensor circuit sensitivity and sensor power dissipation on the load resistance this study was carried out to investigate the dependence of these parameters on the load resistance and justify the selection of the resistance value. Using the sensor electrical equivalent circuit and a hypothetical sensitivity curve, the sensor model equations were developed. From the developed model equations, the equations for the determination of the sensor circuit sensitivity and sensor power loss were derived. The derived equations were used for a particular case of MQ-6 gas sensor under the influence of LPG to plot the graphs of sensor circuit output sensitivity versus load resistance and sensor power dissipation versus sensor resistance from which the trend of variation of sensitivity and sensor power dissipation with the load and the sensor resistance was respectively studied. The appropriate value of load resistance for maximum sensitivity and maximum power loss was determined. The load resistance that yielded maximum sensor circuit sensitivity with the maximum sensor power dissipation less than the set threshold is the candidate resistance for the sensor circuit. The value of the load resistance (20 kΩ.) recommended in MQ-6 datasheet was analytically authenticated in this study.

2. MODELLING OF MQ-SERIES GAS SENSOR CIRCUIT DYNAMICS

The electrical equivalent circuit diagram for MQ-series gas sensors is as shown in Figure 1. V_{CC}, V_{RL}, R_L and R_S are as earlier defined and R_H is the heater resistance. From Figure 1, the current, I flowing through R_S and R_L is given by;

$$I = \frac{V_{CC}}{(R_S + R_L)} \tag{1}$$

The output voltage V_{RL} across the load resistor, R_L, is given by;

$$V_{RL} = \frac{R_L V_{CC}}{(R_S + R_L)} \tag{2}$$

From (2) the resistance R_S is;

$$R_S = \left(\frac{V_{CC}}{V_{RL}} - 1\right) R_L \tag{3}$$

Also, the relationship between the sensor resistance and the gas concentration under a specified environmental condition (temperature and RH) can be obtained from the sensor sensitivity curve present in each of the MQ-series sensor's datasheet. A hypothetical plot of the sensor resistance ratio, $\frac{R_S}{R_O}$ versus the corresponding gas concentration in parts per million (ppm) on the logarithmic scale is shown in Figure 2.
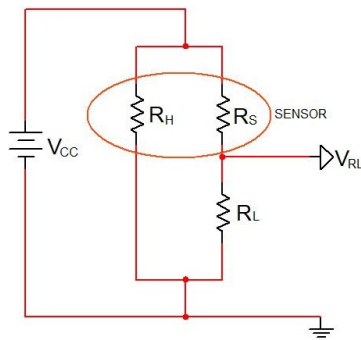

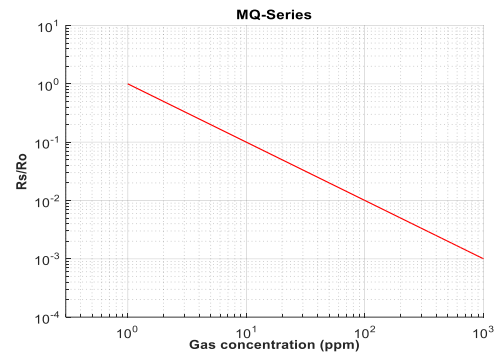Figure 1. MQ-series gas sensor electrical equivalent circuit [30, 31]

Figure 2. Hypothetical MQ-series sensor sensitivity characteristic curve

The sensor resistance ratio and gas concentration were related using the equation of a straight-line graph, Figure 2, obtained as follows:

$$\log_{10}(y) = m \log_{10}(x) + \log_{10}(c) \tag{4}$$

where $y = \frac{R_S}{R_O}$ dimensionless
m = slope of the line
x = gas concentration in ppm
$c = 10^{\wedge(q)}$
where q is the intercept of the line where it cuts the y-axis.

$$m = \frac{\log_{10}(y_2) - \log_{10}(y_1)}{\log_{10}(x_2) - \log_{10}(x_1)} \tag{5}$$

where (x_1, y_1) and (x_2, y_2) are the coordinates of any two different points on the straight line of Figure 2. From (4)

$$c = 10^{\wedge(\log_{10}(y) - m\log_{10}(x))} \tag{6}$$

From (4) the sensor resistance can be expressed in terms of the parameters obtained from the sensitivity curve of Figure 2 as shown in (7).

Analytical determination of load resistance value for MQ-series gas sensors: MQ-6 as … (Ajiboye A. T.)

$$RS = 10^{(m\log_{10}(x)+\log_{10}(c)+\log_{10}(Ro))} \tag{7}$$

Therefore, substituting (7) into (2) gives;

$$V_{RL} = \frac{R_L V_{CC}}{(10^{(m\log_{10}(x)+\log_{10}(c)+\log_{10}(Ro))}+R_L)} \tag{8}$$

3. LOAD RESISTANCE FOR MAXIMUM SENSITIVITY AND SENSOR POWER DISSIPATION

It can be seen from (2) that the output voltage from the sensor circuit that is V_{RL} is a function of V_{CC}, R_S and R_L, but V_{CC} is always constant, therefore, V_{RL} varies only with the value of R_S and R_L. Also, from (7) R_S is a function of x, c and R_O but c is constant, x has a range for a given gas and R_O also has a range for a given class of MQ-series gas sensors. But it should be noted that R_O has a unique value for each member in the class which is normally determined using (3) by empirically measure the value of V_{RL} at a specified value of x and environmental conditions. Based on this, it can be inferred that V_{RL} is a function of x, R_O and R_L. From the MQ-series gas sensor datasheet, the range of R_O and R_L for a particular series of sensors is always specified.

The requirements for the selection of R_L are high output voltage span which will lead to high sensor circuit sensitivity and moderate sensor power dissipation [12]. It should be noted that out of the three parameters on which the value of sensor circuit output voltage (V_{RL}) depends, namely x, R_O and R_L, it is only R_L that can be easily adjusted by the circuit designer to meet the voltage span and power dissipation requirements. This is because x, and R_O are strictly dependent on the inherent characteristics of the gas and sensor material respectively. The sensor output voltage range was determined as follows, from (2) the minimum and maximum output voltage can be expressed as shown in (9-12).

$$V_{RLmin} = \frac{R_L V_{CC}}{(R_{Smas}+R_L)} \tag{9}$$

R_{Smax} is the maximum value of sensor resistance and using (7) is as shown in (10).

$$R_{Smax} = 10^{(m\log_{10}(x_{min})+\log_{10}(c)+\log_{10}(Ro))} \tag{10}$$

where x_{min} is the minimum value of gas concentration in ppm.

$$V_{RLmax} = \frac{R_L V_{CC}}{(R_{Smin}+R_L)} \tag{11}$$

R_{Smin} is the minimum value of sensor resistance and using (7) is as shown in (12)

$$R_{Smin} = 10^{(m\log_{10}(x_{max})+\log_{10}(c)+\log_{10}(Ro))} \tag{12}$$

where x_{max} is the maximum value of gas concentration in ppm. The voltage span was obtained from (9) and (11) and is as expressed in (13)

$$V_{RLspan} = \frac{(R_{Smax}-R_{Smin})R_L V_{CC}}{(R_{Smin}+R_L)(R_{Smax}+R_L)} \tag{13}$$

The sensitivity of the sensor circuit is the ratio of the magnitude of its output voltage span to the corresponding change in the magnitude of the gas concentration and is mathematically expressed in (14).

$$S = \frac{V_{RLspan}}{\Delta x} \tag{14}$$

$\Delta x = x_{max} - x_{min}$ in ppm

The value of R_L that gives the maximum sensitivity for a particular sensor with a given value of R_O can be obtained by plotting S against R_L and determine the value of R_L corresponding to the maximum point of the resulting curve. At maximum sensitivity $R_L = \sqrt{R_{Smin}R_{Smax}}$ [32], therefore, the formula for the power dissipated by the sensor at maximum sensitivity was obtained by multiply the square of the current through the sensor obtained in (1) with the sensor resistance and is as expressed in (15).

$$P_s = \frac{V_{CC}{}^2 R_S}{\left(R_S+\sqrt{R_{Smin}R_{Smax}}\right)^2} \tag{15}$$

Therefore, for a determined value of R_L and given value of R_O, graph of P_S against R_S can be plotted to enable one study the trend of the variation of power dissipated by the sensor with R_S and also, determine the maximum value of the sensor dissipated power at maximum sensitivity. It should be noted that this maximum value must not be greater than the set threshold value given in the sensor manufacturer datasheet [29].

4.   MQ-6 GAS SENSOR CASE STUDY

The MQ-6 gas sensor was selected at random out of many available MQ-series gas sensors. This type of gas sensor is capable of sensing seven gases as listed on the sensitivity curve of Figure 3. Out of these gases, the sensor has a high sensitivity for both LPG and Methane but for this study, LPG was considered. The appropriate value of R_L was determined by first determined the numerical values of the slope m, intercept c, x_{min} and x_{max} and substitute them into the appropriate equation as follows:
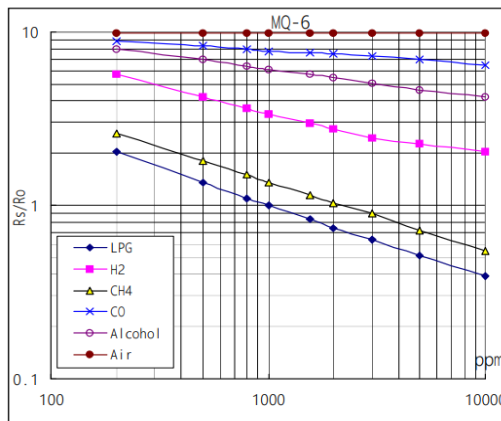

Figure 3. Sensitivity characteristics graph for MQ-6 gas sensor [30, 31]

The slope m was determined by considered two coordinates (200, 2) and (10000, 0.4) on the LPG gas curve on the sensitivity graph of Figure 3. Substituting these coordinates in (5) gives $m = -0.4114$. The parameter c which is embedded in the intercept of the LPG line with the $\frac{R_S}{R_O}$ -axis was determined by selecting the coordinate (1000, 1) on the LPG line on the sensitivity curve, substituting this coordinate value and the value of m in (6) gives $c = 17.1484$. The value of x_{min} and x_{max} for LPG is 200 ppm and 10000 ppm respectively. The relevant parameter values were substituted into (10), (12) (13) and (14) with the value of V_{CC} equal to 5V. After the parameter substitution, (14) was used to plot the graph of S versus R_L for value of R_O increasing from 10 kΩ to 60 kΩ in step of 5 kΩ and the plot yielded the graph of Figure 4. Also, using (15), the graph of the sensor dissipated power versus the sensor resistance was plotted for the obtained value of R_L for the maximum sensitivity and a given value of R_O. The graph was plotted for different values of R_O varying from 10-60 kΩ in step of 5 kΩ and is as shown in Figure 5.
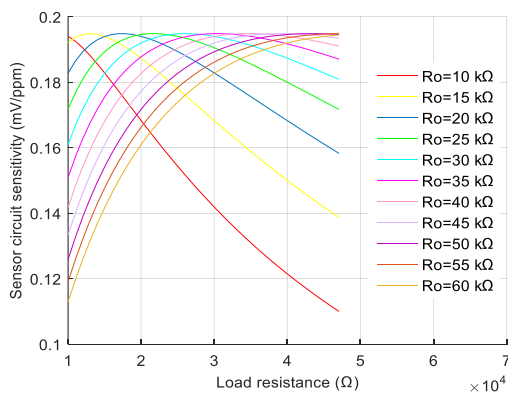

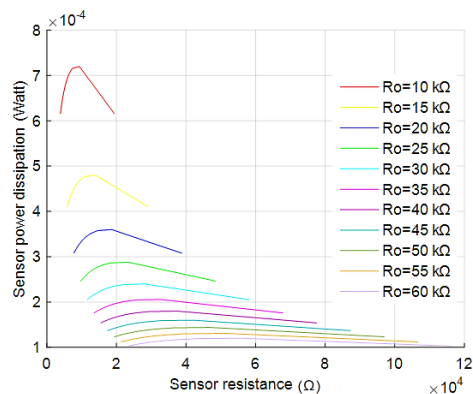Figure 4. Plots of sensor circuit sensitivity versus load resistance for varying values of R_O

Figure 5. Plots of sensor power dissipation versus sensor resistance for varying values of R_O

To test the applicability of this study, the recommendation of R_L=20 kΩ for the MQ-6 sensor in the datasheet [31] was authenticated. The equation that relates R_O and R_L is given in (16).

$$R_O = 10^{((\log 10(R_L{}^2) - m(\log 10(x_{min}) + \log 10(x_{max})) - 2\log 10(c))/2)} \tag{16}$$

Substituting R_L=20 kΩ and the value of other parameters into (16) gives the value of R_O to be 23.065 $k\Omega$. The value of R_O obtained can be confirmed as follows: From the LPG sensitivity curve, for R_S to be equal to R_O the gas concentration must be 1000 ppm. Substitute $m = -0.4114$, $c = 17.15$, R_O=23.065 kΩ and $x = 1000$ ppm into (7) gives Rs=23.065 kΩ. This implies that for this sensor R_O=23.065 kΩ. This shows that the value of R_O for the sensor used in the datasheet is 23.065 $k\Omega$ and for the maximum sensitivity to be obtained R_L must be equal to 20 kΩ which is validated as seen in Figure 6. The plot of the sensor dissipated power against R_S for R_O=23.065 kΩ and R_L=20 kΩ is as shown in Figure 7. From Figure 7, the maximum power dissipated and the value of R_S for maximum power dissipation can be obtained.
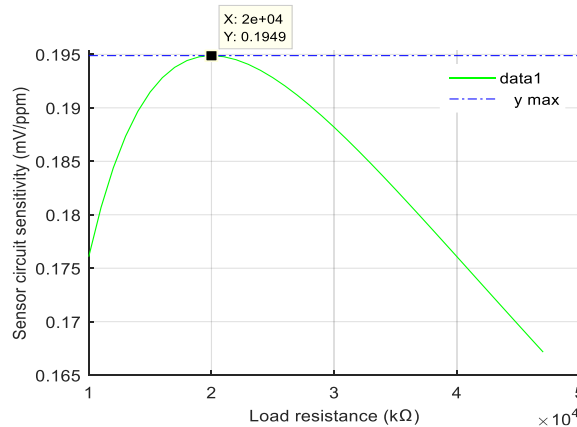

Figure 6. The plot of MQ-6 sensor circuit sensitivity versus load resistance for R_O=23.065 kΩ

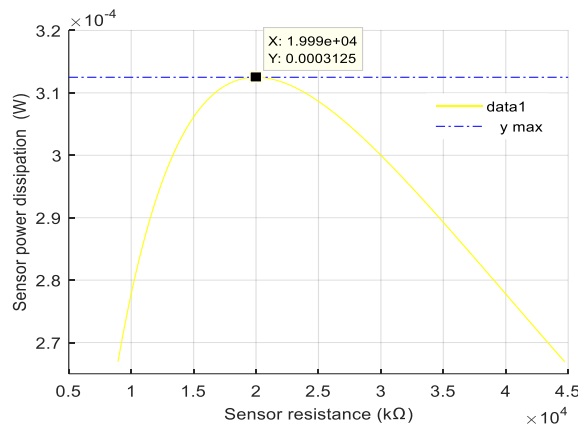Figure 7. The plot of MQ-6 sensor power dissipation against sensor resistance for R_O=23.065 kΩ

5. RESULTS AND DISCUSSION

The data presented in Table 1 were obtained from Figure 4. As can be seen from the figure, the maximum obtainable sensor circuit sensitivity remains fairly constant for different values of R_O from 10-60 kΩ, but the maximum value occurred at different values of R_L for each of the R_O. The value of R_L increases when R_O falls between 10 kΩ and 50 kΩ but remain constant when R_O is between the value of 55 kΩ and 60 kΩ. From this analysis, it is obvious that the obtained value of sensor circuit sensitivity is a function of both the R_O and R_L but it should be noted that R_O is solely depend on the sensor characteristics it is only R_L that can be adjusted by the circuit designer to achieve the required sensitivity.

The data of Table 2 were extracted from Figure 5. It is very clear from the table that the sensor power dissipation decreases as the value of R_O and R_S increases. The highest obtained sensor power dissipation was 7.198×10^{-4} W which is far less than the maximum limit of 15×10^{-3} W [29]. As can be seen from Tables 2, the values of R_L and R_S are approximately equal, which implies that the law of maximum power dissipation is obeyed.

It can be deduced from Tables 1 and 2 that the behaviour of the MQ-6 gas sensor is consistent in terms of maximum sensor circuit sensitivity and sensor power dissipation when R_O is between 10-60 kΩ. The manufacturer of this category of sensor should work toward achieving a high value of R_O because sensor power dissipation decreases with an increase in R_O without affecting the sensor circuit sensitivity. The applicability of this study is confirmed as shown in Figures 6 and 7, where R_O=23.065 kΩ; the maximum sensor's circuit sensitivity and power dissipation are approximately 0.195 mV/ppm and 3.125×10^{-4} W (far less than the maximum limit of 15×10^{-3} W [29]), respectively for R_L=20 kΩ.

Table 1. Maximum sensor circuit sensitivity for a given R_O and the corresponding value of R_L

S(mV/ppm)	R_O (kΩ)	R_L (kΩ)
0.194	10,000	10,000
0.195	15,000	13,000
0.195	20,000	17,000
0.195	25,000	22,000
0.195	30,000	26,000
0.195	35,000	30,000
0.195	40,000	35,000
0.195	45,000	38,000
0.195	50,000	43,000
0.195	55,000	47,000
0.195	60,000	47,000

Table 2. Maximum sensor power dissipation for a given R_O and the corresponding value of R_L

$P_{Smax} \times 10^{-4}$ (W)	R_O (kΩ)	R_S (kΩ)
7,198	10,000	9,340
4,799	15,000	14,000
3,599	20,000	18,680
2,879	25,000	23,350
2,399	30,000	28,030
2,057	35,000	32,700
1,799	40,000	37,370
1,600	45,000	42,040
1,440	50,000	46,710
1,309	55,000	51,380
1,200	60,000	56,050

6. CONCLUSION

The sensor circuit dynamics was modelled and the developed model equations were used for determining, for a given R_O: (i) sensor circuit sensitivity as a function of load resistance and (ii) sensor power dissipation as a function of sensor resistance. The highest sensor power dissipation obtained when Ro = 10 kΩ was 7.198×10^{-4} W (<< the maximum limit of 15×10^{-3} W). It can be deduced from the study that the MQ-6 gas sensor has consistent behaviour in terms of maximum sensor circuit sensitivity and sensor power dissipation when 10 kΩ<R_O<60 kΩ. The manufacturer of this category of sensor should increase the value of R_O as the level of sensor power dissipation is inversely related to the former. Finally, the 20 kΩ load resistance recommended for MQ-6 in the datasheet was also validated in this study because it gives maximum sensor circuit sensitivity and tolerable sensor power dissipation.

REFERENCES
[1] A. Popa *et al.*, "An intelligent IoT-based food quality monitoring approach using low-cost sensors," *Symmetry,* vol. 11, no. 3, 2019.
[2] H. Baha and Z. Dibi, "A novel neural network-based technique for smart gas sensors operating in a dynamic environment," *Sensors,* vol. 9, no. 11, pp. 8944-8960, 2009.
[3] R. Rumantri, M. Khakim, and I. Iskandar, "Design and Characterization of Low-Cost Sensors for Air Quality Monitoring System," *Jurnal Pendidikan IPA Indonesia,* vol. 7, no. 3, pp. 347-354, 2018.
[4] V. Deotalu, A. Loyare, C. Dandekar, and R. Mandi, "Real-Time Olfaction Monitoring system & Implementation of E-sensing Technique in Electronic Nose," *International Research Journal of Engineering and Technology*, vol. 04, no. 04, pp. 858-863, 2016.
[5] K. V. D. Ambeth, "Human security from death-defying gases using an intelligent sensor system," *Sensing and bio-sensing research,* vol. 7, pp. 107-114, 2016.
[6] Q. Ding, D. Zhao, and Z. Yang, "Detection of fruits in warehouse using Electronic nose," in *MATEC Web of Conferences*, 2018.
[7] J. Y. Kim, S. W. Kang, T. Z. Shin, M. K. Yang, and K. S. Lee, "Design of a smart gas sensor system for room air-cleaner of automobile-thick-film metal oxide semiconductor gas sensor," *2006 International Forum on Strategic Technology,* pp. 72-75, 2006.
[8] A. Kanade and A. Shaligram, "Development of an E-Nose using metal oxide semiconductor sensors for the classification of climacteric fruits," *International Journal of Scientific & Engineering Research,* vol. 5, no. 2, 2014.
[9] J. Chilo, J. Pelegri-Sebastia, M. Cupane, and T. Sogorb, "E-nose application to food industry production," *IEEE Instrumentation & Measurement Magazine,* vol. 19, no. 1, pp. 27-33, 2016.

[10] K. Vandana and C. Baweja, "Simmarpreet, and S. Chopra, "Influence of Temperature and Humidity on the Output Resistance Ratio of the MQ-135 Sensor," *Int. J. Adv. Res. Comput. Sci. Softw. Eng,* vol. 6, no. 4, pp. 423-429, 2016.

[11] H. Baha and Z. Dibi, "Ann modeling of a gas sensor," *Journal of Electrical Engineering and Technology,* vol. 5, no. 3, pp. 493-496, 2010.

[12] K. Lamamra and D. Rechem, "Artificial neural network modelling of a gas sensor for liquefied petroleum gas detection," in *2016 8th International Conference on Modelling, Identification and Control (ICMIC)*, 2016, pp. 163-168.

[13] M. Fezari, R. Hattab, And A. Al-Dahoud, "Oak Ridge Air Quality Index Computation: a way for Monitoring Pollutions in Annaba City," *Conference: International Arab Conference on Information Technology (ACIT)*, 2015.

[14] S. Kouda, A. Dendouga, S. Barra, and T. Bendib, "Design of a selective smart gas sensor based on ANN-FL hybrid modeling," *Journal of Nano- and Electronic Physics,* vol. 10, no. 6, pp. 06011-1-06011-5, 2018.

[15] Z. Nenova and G. Dimchev, "Compensation of the impact of disturbing factors on gas sensor characteristics," *Acta Polytech. Hung,* vol. 10, no. 3, pp. 97-111, 2013.

[16] A. Shahid, J.-H. Choi, A. U. H. S. Rana, and H.-S. Kim, "Least-Squares Neural Network-Based Wireless E-Nose System Using an SnO2 Sensor Array," *Sensors,* vol. 18, no. 5, p. 1446, 2018.

[17] Q. A. Al-Haija, H. Al-Qadeeb, and A. Al-Lwaimi, "Case Study: Monitoring of AIR quality in King Faisal University using a microcontroller and WSN," *Procedia Computer Science,* vol. 21, pp. 517-521, 2013.

[18] B. B. L. Heyasa and R. G. Van Ryan Kristopher, "Initial Development and Testing of Microcontroller-MQ2 Gas Sensor for University Air Quality Monitoring," *IOSR Journal of Electrical and Electronics Engineering (IOSR-JEEE),* vol. 12, no. 3, pp. 47-53, 2017.

[19] A. Biswal, J. Subhashini, and A. K. Pasayat, "Air quality monitoring system for indoor environments using IoT," *AIP Conference Proceedings*, 2019, vol. 2112, no. 1, p. 020180: AIP Publishing LLC.

[20] H. A. H. Nograles, C. P. D. Agbay, I. S. L. Flores, A. L. Manuel, and J. B. C. Salonga, "Low-cost internet-based wireless sensor network for air pollution monitoring using Zigbee module," *2014 Fourth International Conference on Digital Information and Communication Technology and its Applications (DICTAP)*, 2014, pp. 310-314.

[21] S. N. Mahmood, A. J. Ishak, and S. T. Hussain, "GSM based gas leak monitoring system," *Periodicals of Engineering and Natural Sciences,* vol. 7, no. 2, pp. 670-678, 2019.

[22] S. Natarajan, P. Deshpande, P. Gole, and P. Bhosale, "LPG Gas Detector and Prevention," *International Journal of Current Research,* Journal vol. 9, no. 10, pp. 60140-60142, 2017.

[23] M. Aishwarya.A., M. R. B.N, and K. Prasad.R, "LPG Gas Leakage Detection and Prevention System," *International Journal on Future Revolution in Computer Science & Communication Engineering (IJFRCSCE),* vol. 3, no. 8, pp. 01-04, 2017.

[24] Z. Chafekar, M. H. Khan, K. Lakra, and S. Dhonde, "Implementation of Automatic Gas Accident Prevention System using Arduino and GSM," *International Journal of Computer Applications,* vol. 180, no. 47, pp. 5-7, 2018.

[25] K. B. Suarsana, A. A. N. Gunawan, and N. N. Ratini, "LPG Leakage Control Using SMS through SIM800L with MQ-2 Sensor and Stepper Motor Based on Arduino UNO," *Advances in Applied Physics*, vol. 6, no. 1, pp. 15-18, 2018.

[26] T. Ismail, D. Das, J. Saikia, J. Deka, and R. Sarma, "GSM based gas leakage warning system," *International Journal of Advanced Research in Computer and Communication Engineering,* vol. 4, no. 3, pp. 6293-6298, 2014.

[27] A. Suyuti, A. Ahmad, And A. Ejah Umraeni Salam, "Intelligent System of LPG Gas Leakage Detection for Web-Based Living House Security," *ICIC express letters. Part B, Applications: an international journal of research and surveys,* vol. 10, no. 2, pp. 89-96, 2019.

[28] M. W. Siddiqui and K. M. Mishra, "LPG Leakage Detection and Prevention," *Imperial Journal of Interdisciplinary Research (IJIR),* vol. 3, no. 5, pp. 1084-1086, 2017.

[29] S. M. Hadi, W. R. Abdulmajeed, M. M. Thib, and U. Baghdad, "Design and Implement a Gas Pipeline Inspection System using Robotic Vehicle," *Journal of Information Engineering and Applications,* vol. 4, no. 9, pp. 49-56, 2014.

[30] Winsen, "Flammable Gas Sensor (Model: MQ-6)," in *www.winsensor.com*, L. Zhengzhou Winsen Electronics Technology Co., Ed., ed. China: Zhengzhou Winsen Electronics Technology Co., Ltd, pp. 1-7, 2014.

[31] Hanwei, "Technical Data MQ-6 Gas Sensor," in *www.hwsensor.com*, H. Sensors, Ed., ed. China: Hanwei Sensors, pp. 1-2, 2019.

[32] Z. Liu, "Automatic Control for a Gas System Using PIC Microcontroller," Bachelor Program in Electronics Bachelor, Faculty of Engineering and Sustainable Development, University of Gavle, Sweden, 2013.